https://doi.org/10.5194/egusphere-2025-3873
Preprint. Discussion started: 5 September 2025

Natural Methane Emissions Feedbacks in MAGICC v. 7.6

Trevor Sloughter[1], Zebedee Nicholls[2], Gang Tang[3], Thomas Kleinen[4], Zhen Zhang[5], and Joeri Rogelj[1,2,6]

[1]Centre for Environmental Policy, Imperial College London, SW20 8RP London, United Kingdom
[2]International Institute for Applied Systems Analysis, A-2361 Laxenburg, Austria
[3]University of Melbourne, Parkville VIC 3010, Melbourne, Australia
[4]Max Planck Institute for Meteorology, 20146 Hamburg, Germany
[5]Institute of Tibetan Plateau Research, Chinese Academy of Sciences, 100101 Beijing, China
[6]Grantham Institute for Climate Change and the Environment, Imperial College London, SW7 2AZ London, United Kingdom

Correspondence: Trevor Sloughter (t.sloughter@imperial.ac.uk)

Abstract. Literature estimates of natural methane emissions, particularly from wetlands, have a wide range of uncertainty. Meanwhile, few Earth System Models (ESMs) explicitly model wetlands as a potential source of methane. As a result, Simple Climate Models that aim to emulate the behaviour of ESMs have little to constrain their present and future contributions. MAGICC, as of version 7.5.3, fixed natural methane concentrations as constant after the historical period. Two studies that model wetland methane emissions over the 21^{st} century both find a relationship between those emissions and global temperature, though disagree on the extent of this temperature sensitivity. An updated version of MAGICC has been created that uses this evidence to include a linearised representation of the relationship between wetland methane emissions and global temperature. The temperature-sensitivity parameter in this relationship has been parametrised in a way such that its distribution encompasses the uncertainty in both modelling literature and carbon budget studies, reflecting the currently high degree of uncertainty in wetlands emissions. Our results show how incorporating a temperature feedback in methane emissions leads to both higher temperature projections for all scenarios used here, and a widening of the uncertainty in global temperature response.

1 Introduction

Globally, wetland area has been estimated at around 12 million km^2 (Davidson et al., 2018), nearly 8% of Earth's land surface area. With their emissions accounting for anywhere between 20% and 30% of all global natural and anthropogenic methane emissions (Saunois et al., 2020; Zhang et al., 2025), wetlands are the largest source of methane emissions in the coupled Human-Earth System (Gedney et al., 2019), and potentially represent important components of the Earth system for modelling future climate. However, as yet few Earth System Models (ESMs) explicitly model wetlands.

One ESM which did incorporate a wetlands module (Kleinen et al., 2021a) reported CH_4 emissions from wetlands alone rivalling, or in some scenarios even overtaking, anthropogenic sources within the next century. This was attributed in large

https://doi.org/10.5194/egusphere-2025-3873
Preprint. Discussion started: 5 September 2025

part to the rise in temperature spurring greater productivity in wetlands, as well as changing precipitation inundating a larger land area, resulting in this substantial additional methane source. Increased inundation has also been reported as a cause of increased emissions in recent years (Qu et al., 2024). Wetland methane emissions are partially dependent on temperature, but due to the other drivers mentioned, which are themselves partially dependent on temperature, emissions do not necessarily follow the same trajectory with decreasing temperatures as they do with increasing temperatures. This potential hysteresis was noted on seasonal time scales (Chang et al., 2021).

Wetland methane surface models often reproduce the historical period, incorporating measurement data to attempt estimates of the current emission rates, and few project future trends over the next century (Peng et al., 2022; Skeie et al., 2023; Zhang et al., 2023). Feedbacks are easier to detect in future projections than in historical simulations, and without more models of 21st century wetland methane there are limits to how simple climate models (SCMs) can be calibrated. To date, most SCMs do not incorporate explicit derivation of wetland feedbacks, although some are adding modules that capture related processes, such as OSCAR adding a peatland component (Zhu et al., 2024). One such SCM, the Model for the Assessment of Greenhouse-gas-Induced Climate Change (MAGICC) (Meinshausen et al., 2011a), had previously not incorporated dynamic natural methane in its future projections, instead taking historical concentrations up to the present, after which natural methane is kept constant (Meinshausen et al., 2011a, 2020).

MAGICC is particularly relevant as it is used to prepare concentration inputs for ESM experiments from the scenario emissions data, such as those in ScenarioMIP (O'Neill et al., 2016; Riahi et al., 2017). Kleinen et al. (2021a) cite the risk of CMIP potentially greatly under-estimating natural methane emissions, with wetlands being the largest single source in their results. Here we present a version of MAGICC which incorporates an approximation of the effect of wetlands on natural methane emissions as found in two global models for the period up to 2100 and beyond.

2 Methods

2.1 Methane Data

Projections of wetland methane emissions were taken from two prior modelling studies. One, Kleinen et al. (2021a), added a wetlands component to the Max Planck Institute for Meteorology Earth System Model (MPI-ESM) (Mauritsen et al., 2019). The other, Zhang et al. (2017), used a wetlands model whose emissions were fed into MAGICC v. 6 to calculate global temperatures, which were then fed back into the wetlands model. Kleinen et al. ran their modified ESM for several scenarios based on the Shared Socioeconomic Pathways (SSPs), SSP1-1.9, SSP1-2.6, SSP2-4.5, SSP3-7.0, and SSP5-8.5 up to 2100 and then extended by Kleinen *et al.* to the year 3000, following the same method that had been used in Meinshausen et al. (2020) to extend them to 2500. Zhang et al. used the older Representative Concentration Pathways RCP2.6, RCP4.5, and RCP6.0 and RCP8.5 (Meinshausen et al., 2011b). For issues of data availability, when calibrating to Zhang et al. (2017), this study uses only RCP2.6 and RCP8.5.

https://doi.org/10.5194/egusphere-2025-3873
Preprint. Discussion started: 5 September 2025

2.1.1 Model & Calibration

Both available papers on wetland methane emissions found a strong linear correlation between emissions and global temperature in their models. Shown in Figure A3 are the annual methane emissions, averaged using a 50-year running mean, against global temperature anomaly up to the year 2300 in Kleinen et al. (2021a).

The aforementioned linear relationship between wetland methane emissions and global temperature holds in the cited models at least for the next century. Beyond 2300, as global temperatures stabilise, wetland methane emissions decrease in the MPI-ESM, and thus the linear model no longer fits. This can be seen in Figure 2 of Kleinen et al. (2021a), which is reproduced in Figure A1 here. This nonlinear effect is also evidence when comparing the scatter plots shown in Figure A2 which use all the data up to the year 3000, versus the scatter plot in A3 only taking data up to 2500. The nonlinear effects are much less prominent in the near centuries than further into the millennium. And, as mentioned above and described by the authors, with every additional century the uncertainty in the results increases.

For this reason, here we model wetland methane emissions (E_ϕ^n) as a linear function of the global average temperature anomaly T with a slope m and intercept E_0:

$$E_\phi^n = mT + E_0 \tag{1}$$

This equation was then fit to the available data using the Nelder-Mead method and a cost function calculating the root mean-squared error (RMSE). The Kleinen et al. (2021a) time series extends up to the year 3000, but the authors express increasing degrees of uncertainty beyond 2300. Equation 1 was calibrated using the full time series up to 3000, but also using subsets ending at 2500 and 2300.

The model was fit to each dataset separately, one calibration simultaneously fitting to the five SSPs in (Kleinen et al., 2021a), and the other to the two RCPs for (Zhang et al., 2017).

These calibrations of slope m to the available simulation data from Kleinen et al. (2021a) and Zhang et al. (2017) were used to define a normal distribution. Values from Kleinen et al. (2021a) were assumed to be on the high end of sensitivity due to evidence from ensemble estimates of wetland emissions from 2000-2020 (Zhang et al., 2025) and more recent 21st century simulations (Im et al., 2025). Although those studies weren't usable for calibration, they suggest lower temperature sensitivities are also reasonable. Therefore, the distribution was given a median of 30 Mt/K with a standard deviation of 13 Mt/K. Thus the slope derived from Kleinen et al. (2021a) falls within 2 standard deviations of the mean, which is near the slope derived from Zhang et al. (2017). This setup is also consistent with temperature sensitivities of wetland emissions found in an analysis of 16 process-based models (Zhang et al., 2025). This distribution thus encompasses the wide uncertainty range applicable to the quantification of this effect. The lower bound is not clearly constrained in this framework, but is consistent with a more recent study that was published after the above analysis (Im et al., 2025). That study also modelled wetlands and other natural sources of methane into the future, but did not find a strong temperature sensitivity, and hence there was little to no increase in wetlands emissions over the next century. This suggests that modelling estimates of temperature sensitivity do indeed span a range from near zero to the high end of Kleinen et al. (2021a)

https://doi.org/10.5194/egusphere-2025-3873
Preprint. Discussion started: 5 September 2025

Here, MAGICC, both with and without wetland methane, is concentration-driven until 2015 when it switches to emissions-driven. Thus, after 2015 is also when the natural methane emissions are calculated with Equation 1, allowing for historical methane to be constrained by observational data. This also serves to fix the intercept E_0 so that the transition is continuous. The resulting version with wetlands methane is MAGICC v7.6.0 (Nicholls et al., 2025).

2.2 Scenario Experiments

Both the new MAGICC and the previous version (v. 7.5.3) were run with the IPCC AR6 scenarios in categories C1, C2 and C3 (Byers et al., 2022; Kikstra et al., 2022), to compare the effects of emissions generated by Equation 1. The categories are defined with respect to the limits of either their peak warming or their end-of-century (EOC) warming in the case of overshoot. The first category, C1, are scenarios defined as reaching or exceeding "1.5°C during the 21st century with a likelihood of $\leq$67%, and limit warming to 1.5°C in 2100 with a likelihood $>$50%. Limited overshoot refers to exceeding 1.5°C by up to about 0.1°C and for up to several decades" (Riahi et al., 2022). The second, C2, is defined similarly but allowing for higher overshoot, these scenarios "[e]xceed warming of 1.5°C during the 21st century with a likelihood of $>$67%, and limit warming to 1.5°C in 2100 with a likelihood of $>$50%. High overshoot refers to temporarily exceeding 1.5°C global warming by 0.1°C–0.3°C for up to several decades". The third, C3, are scenarios which "[l]imit peak warming to 2°C throughout the 21st century with a likelihood of $>$67%" (*ibid*).

Both versions of MAGICC were run from 1750 to 2105 (Meinshausen et al., 2020), using a probabilistic approach with 600 draws of parameter combinations for each scenario (Sloughter and Nicholls, 2025). The runs were concentration-driven up to 2015, using the same historical data previously described in Nicholls et al. (2021), before switching to emissions-driven scenarios from 2015 onward.

3 RESULTS

3.1 Parametrisation

Temperature sensitivity calibrated using the Zhang et al. (2017) data was 35.5 Mt CH_4/K. Calibrating to the full Kleinen et al. (2021a) data, up to the year 3000, resulted in a temperature sensitivity of 37.5 Mt CH_4/K. This is a lower slope for Equation 1 than if the calibration only used data up to the year 2500, giving a slope of 45.8 Mt CH_4/K, or to 2300, with a slope of 52.6 Mt CH_4/K (see also Table A1). Considering the aforementioned high uncertainty beyond 2300, the nonlinearity after this point, and the focus of these experiments on this century, the higher estimate of 52.6 Mt/K was used to inform the higher end of the parameter distribution for the linear model.

MAGICC v7.6 draws slopes from a normal distribution with a mean of 30 Mt/K, and a standard deviation of 13 Mt/K. This kept the majority of slopes near to the estimate derived from Zhang et al. (2017) while allowing for a number to extend above the Kleinen et al. (2021a) fit on the high end.

https://doi.org/10.5194/egusphere-2025-3873
Preprint. Discussion started: 5 September 2025

3.2 Emissions and Concentrations

The new version of MAGICC has higher natural methane emissions. Even in cooler scenarios, such as SSP1-2.6, CH_4 emissions rise to over 200 Mt/yr by the middle of the century in the new model, an increase of over 20 Mt/yr relative to the older version's constant emission rate of ∼182 Mt/year in the 21^{st} century. Warmer temperatures necessarily lead to higher emissions, with median peak natural methane emissions rising above 216 Mt/K in C3 scenarios, and as high as 265.8 Mt/yr in the 95^{th} percentile of emissions.

Figure 1 shows atmospheric concentrations of carbon dioxide and methane, as well as the annual natural CH_4 emissions from the simulation of the SSP1-2.6, SSP2-4.5 and SSP3-7.0 scenarios. MAGICC v7.5.3's natural emissions are constant. Emissions are converted into concentrations according to the same carbon and methane processes described in Meinshausen et al. (2011a), which remained unchanged in v7.6. These emission differences result in the higher CH_4 concentrations in MAGICC v7.6 than MAGICC v7.5. This also leads to the higher CO_2 concentrations in the new model version as a result of the increased CH4 oxidation and the increased CO_2 respiration (under higher temperature)." The result, also shown in the examples in Figure 1, is an increase in atmospheric methane following rising temperatures. There is also a small increase in carbon dioxide concentrations, on the order of a few ppm, as a result of climate-carbon feedbacks at higher temperatures.

3.3 Temperatures and Scenarios

As the new model necessarily includes higher methane emissions from the addition of wetlands, all scenarios see higher atmospheric methane concentration and subsequently higher temperatures across the next century. This is most evident in comparing the peak and end-of-century (EOC) temperatures. Figure 2a shows the amount of increase in peak and EOC temperatures in v7.6 plotted against the amount of peak and EOC warming in v7.5.3, for scenarios in the AR6 categores C1-3. Figure 2b compares the relative change in peak versus EOC temperatures. Both demonstrate that not only are all scenarios warmer in v7.6, but the warmer a scenario was previously, the greater its increase in temperature with the added wetlands feedback. Figure 2d illustrates the slight decrease in total drawdown in the newer version. Drawdown, defined here as the difference between the peak and end-of-century warming, is slightly weaker for warmer scenarios.

Moreover, the uncertainty in global temperature also increases. Figure 2d plots the differences, for each scenario, between the temperatures in 2100 for the 95^{th} and 5^{th} percentiles, for both versions of MAGICC. Not only are the temperatures warmer, but the range between these extremes widens with warmer scenarios. Higher uncertainty in v7.5.3 leads to even higher uncertainty in v7.6, roughly ten percent higher. Figure 2e shows how EOC temperatures in v7.6 compare to v7.5.3 as a ratio, for both the 5^{th} and 95^{th} percentiles, demonstrating how both the lower and higher end of temperature estimates increase in v7.6.

As a result, all scenarios have a higher probability of exceeding 2°C. While the overall impact on peak temperature is on the order of a few hundredths to a tenth of a degree Celsius, this pushes a number of scenarios above 2° in this percentile.

When run with MAGICC v7.6, nine of the 97 C1 scenarios exceed the EOC warming limit of 1.5°C with a greater than 50% probability. These scenarios would then be more in line with the C3 category as their peak warming would still not have a greater than 33% probability of exceeding 2°C. Of the 133 C2 scenarios, 33 no longer stay below 1.5°C warming at the end

https://doi.org/10.5194/egusphere-2025-3873
Preprint. Discussion started: 5 September 2025

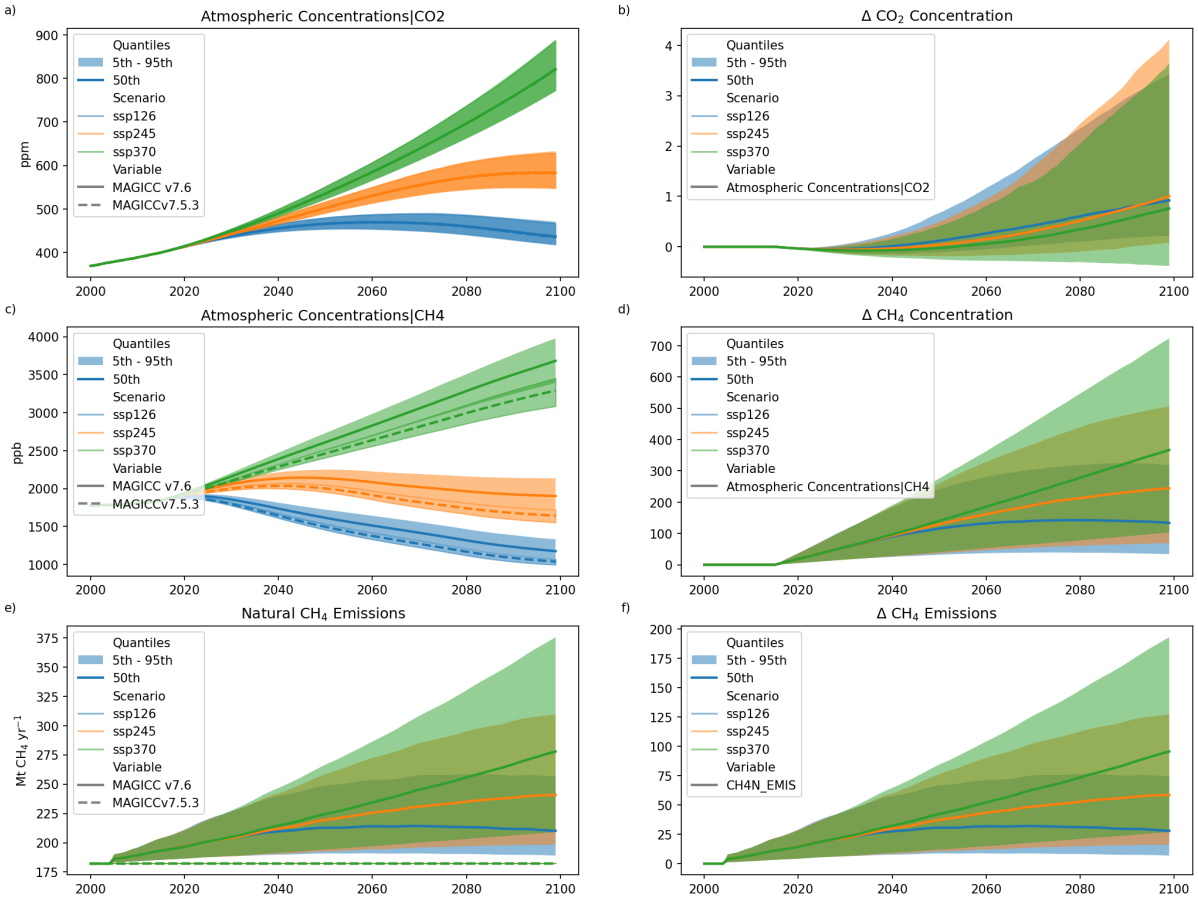

Figure 1. Left column: Comparisons of the atmospheric CO_2 and CH_4 concentrations and natural CH_4 emissions between in MAGICC v7.5.3 (dashed lines) and v7.6 (solid lines) for three SSP scenarios. Right column: The differences between versions in concentrations of CO_2 and CH_4 and natural emissions of CH_4. As the older version of MAGICC held natural methane sources constant, it has a flat line in the emissions plot.

https://doi.org/10.5194/egusphere-2025-3873
Preprint. Discussion started: 5 September 2025

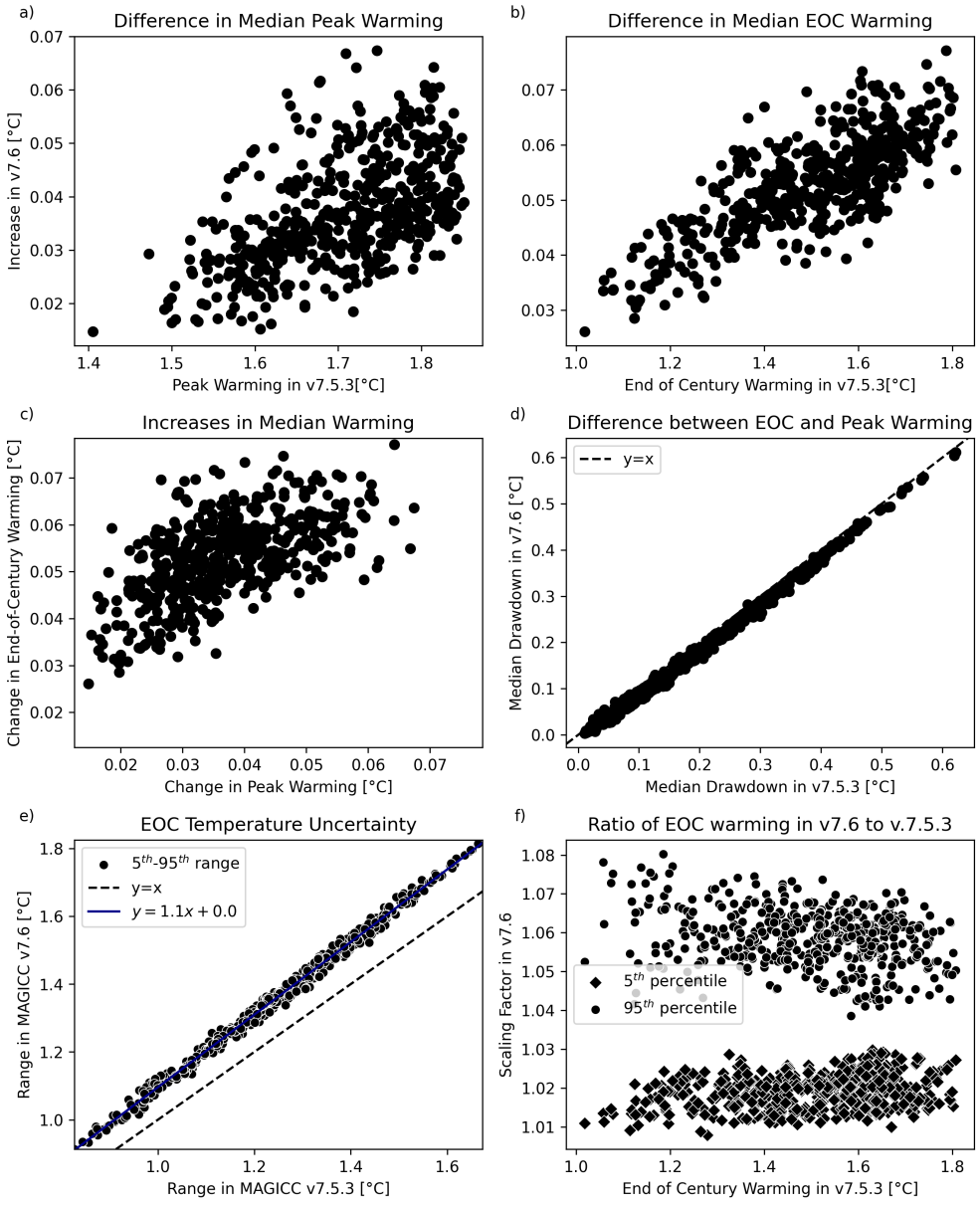

Figure 2. Comparisons of the changes to peak and end-of-century (EOC) warming in MAGICC v7.6 when compared with v7.5.3. Top left: The increase in peak temperatures between model versions plotted against the peak warming in v7.5.3 Top right: The increase in EOC temperatures between model versions lotted against EOC warming in v7.5.3. Middle left: The increase in peak temperatures plotted against the increase in EOC tempreatures. Middle right: Drawdown, the difference between peak and EOC temperatures, for v7.6 plotted against drawdown in v7.5.3. Bottom left: The range of EOC temperatures between the 5^{th} and 95^{th} percentiles for v7.6 plotted against those ranges for for v7.5.3. Bottom right: The ratio of EOC temperatures in v7.6 to those in v7.5.3 for the 5^{th} and 95^{th} percentiles.

https://doi.org/10.5194/egusphere-2025-3873
Preprint. Discussion started: 5 September 2025

of the century with a 50% probability. Of those, 130 would still meet the cutoff for C3, The remaining three have a greater than 33% chance of exceeding 2° of warming, though they would still have a 50% probability of remaining below 2°C (the cutoff for the C4 category). Of the 311 C3 scenarios, 82 no longer stay below 2°C warming throughout the century with a 67% probability, but do stay below with a 50% probability. Figure 3 plot the scenarios in each category along with their respective cutoffs.

The C1 and C1 scenarios represent overshoot pathways that return to 1.5°C of warming by the end of the century. In MAGICC v7.5.3, the C1 scenarios have a mean overshoot duration of 28.7 years (standard deviation: 13.7), and C2 scenarios overshoot for a mean of 53.3 years (standard deviation: 10.8). By contrast, in v7.6 the duration of overshoot is longer, with a mean of 38.9 years (SD: 15.9) for C1 scenarios and 59.9 years (SD: 9.9) for C2. As the length of the overshoot period is longer and the temperatures higher, so too is the integral of the temperature curve exceeding 1.5°C, expressed in degree-years, is also increased. In v7.5.3 the means are 1.5 (SD: 1.0) and 7.0 (SD: 3.1) degree-years for C1 and C2, respectively. In v7.6, the means are 2.7 (SD: 1.6) and 9.3 (SD: 3.6) degree-years for C1 and C2.

4 Discussion

As established, the distribution of the temperature-sensitivity parameters in MAGICC v7.6 encompasses a range of estimates from the modelling literature (Zhang et al., 2017; Kleinen et al., 2021a; Im et al., 2025). The resulting wetland methane emissions are consistent with results from modelling studies such as Folberth et al. (2022), as well as the wide range of estimated methane emissions in the present estimated in the Global Methane Budget (GMB) (Saunois et al., 2024). The average bottom-up estimate of global wetland methane emissions between 2010 and 2019 is 165 Mt/yr. The top-down estimate for the same time period, which also include emissions from inland waters, has a mean of 248 Mt/yr. The median temperature sensitivity in MAGICC v7.6 leads to wetland methane emissions estimates in between these two values in the GMB (Saunois et al., 2020), close to 200 Mt/yr for most scenarios in the 2015-2019 period. Likewise, the upper and lower bounds of temperature sensitivity align with the upper and lower GMB emissions estimates.

While the change in emissions is noticeable, the effect on temperature is smaller. Peak and end-of-century temperatures are higher across all scenarios, by a few hundredths of a degree Celsius, and hence this affects scenario categorisation and projections of the magnitude and length of temperature overshoot. The magnitude of temperature increase may be small for any given year, but this can add up to many years longer of overshoot.

With the limited number of models at hand for calibration, there is a risk of results being skewed. Additionally, Kleinen et al. (2021a) notes the many processes that affect wetland emissions are entangled with temperature. Changes in precipitation and the expansion of tropical wetland area were large drivers of increasing emissions in their study, while here we use temperature only as a proxy for all of these. This is one of the reasons that in the latter half of the millennium, wetland emissions decrease even as temperatures stabilise. The model in this paper is reversible, decreasing temperatures decreases wetland emissions, but this is a simplification. In Kleinen et al. (2021a), the linear relationship between wetland methane and surface warming holds even in overshoot scenarios, where temperatures decline after a peak, for the next century, but extending beyond 2100

https://doi.org/10.5194/egusphere-2025-3873
Preprint. Discussion started: 5 September 2025

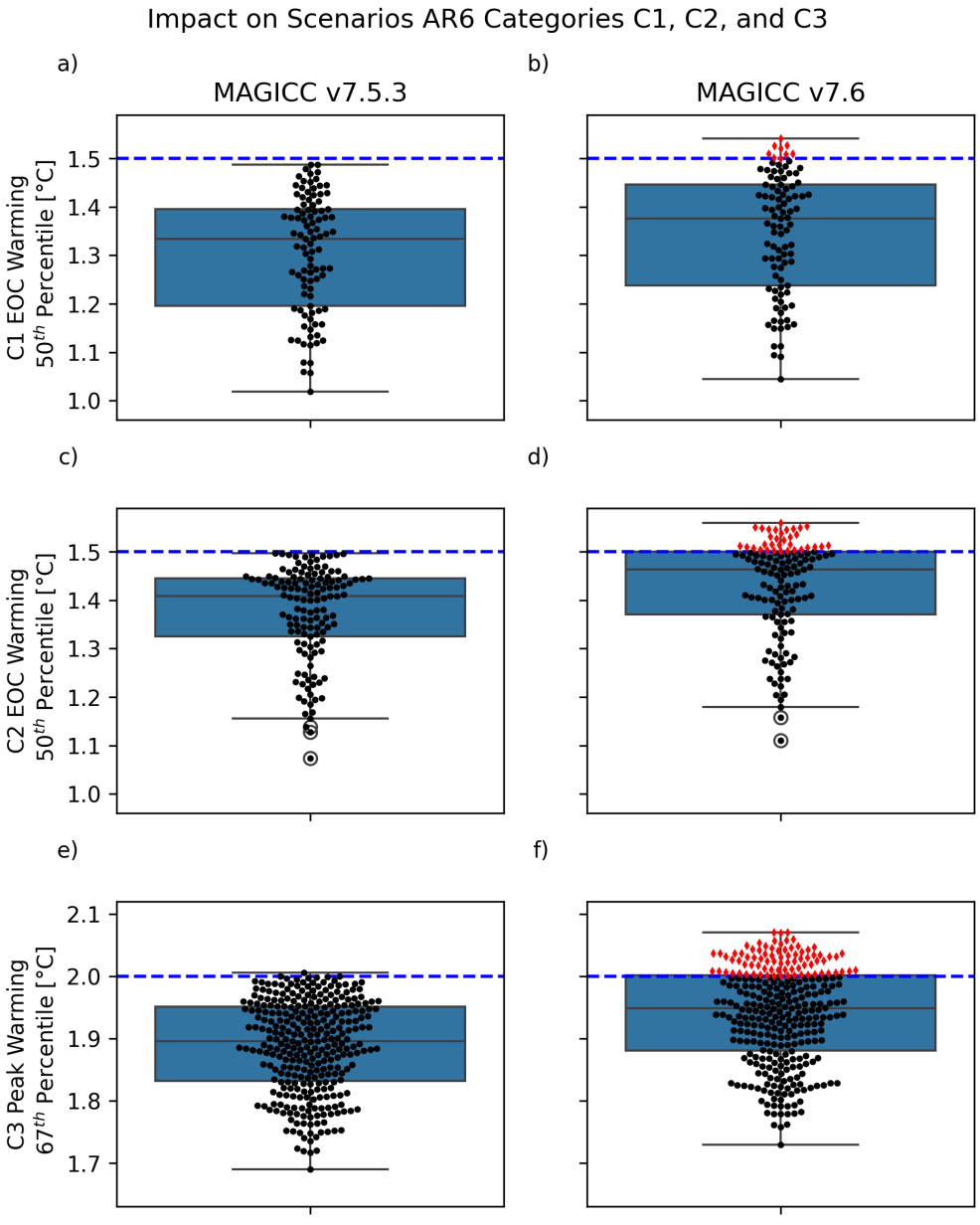

Figure 3. Effect of additional natural methane emissions on scenarios with respect to the AR6 category cutoffs. Top and middle rows show median end-of-century surface air temperature anomalies in each version of MAGICC for the C1 and C2 scenarios. The 1.5°C limit is indicated with the dashed line, and the scenarios in red exceed the limiting definitions of their categories when wetland methane is included. The bottom row shows the 67^{th} percentile peak surface air temperature anomalies for the C3 scenarios. The 2°C limit is indicated with the dashed line, and the scenarios in red exceed this peak warming cutoff which defines the category.

https://doi.org/10.5194/egusphere-2025-3873
Preprint. Discussion started: 5 September 2025

this does not appear to be the case (see also Figures A2c and A3). Beyond 2100, especially for much higher cases of warming, reversibility is in question.

Future research can consider these interdependencies by including variables other than temperature, such as precipitation or wetlands area. However, these are typically not modelled or emulated by current SCMs. More ESMs for calibration would also be invaluable for better parameterisation.

5 Conclusions

We have included a wetland methane feedback, proportional to temperature, in MAGICC. This makes a noticeable difference in projected atmospheric methane concentrations across a range of scenarios over the next centuries. For mitigation scenarios assessed in AR6, the rise in methane concentrations leads to a small increase in temperature on the order of a hundredth of a degree Celsius at the peak. This temperature change is small, but nevertheless affects the number of scenarios that initially projected to return warming below 1.5°C with at least 50% probability in 2100 or those limiting warming to 2°C.

MAGICC is being used for CMIP7's boundary conditions, and will ensure that the low bias, from having assumed constant natural methane emissions previously in CMIP6, is not repeated. While these boundary conditions will be imperfect both in hindsight and for the reasons already discussed above, this progress will be strengthened by the new insights that are expected from CMIP7-generation models.

https://doi.org/10.5194/egusphere-2025-3873
Preprint. Discussion started: 5 September 2025

Appendix A

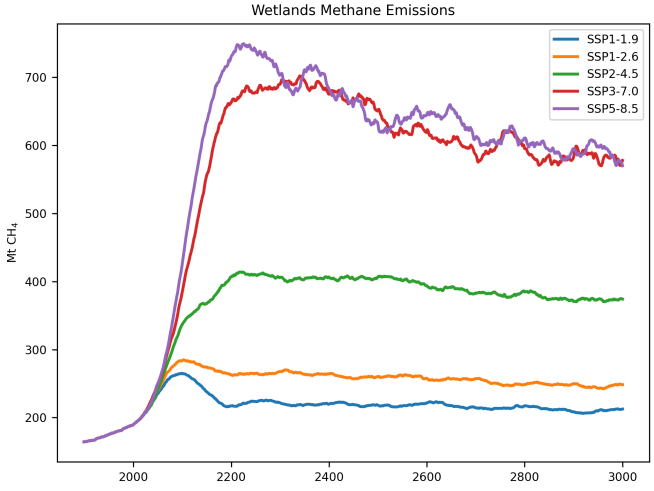

Figure A1. 50-year running mean of Wetland methane emissions, reproduced from Figure 2 in Kleinen et al. (2021a).

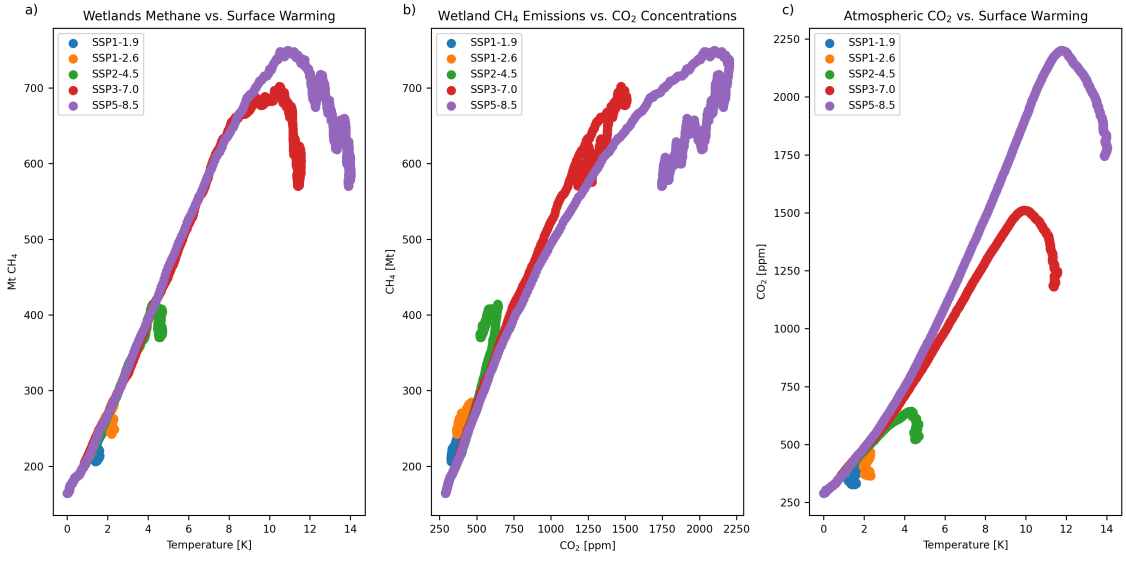

Figure A2. Relationships between wetland methane emissions, atmospheric carbon dioxide concentrations, and surface warming from 1850 to 3000 in Kleinen et al. (2021a).

https://doi.org/10.5194/egusphere-2025-3873
Preprint. Discussion started: 5 September 2025

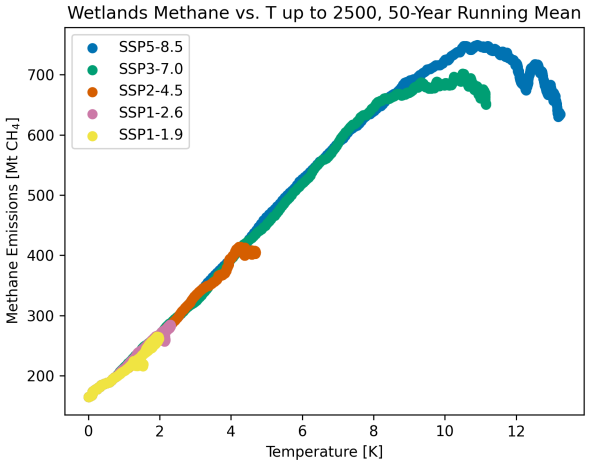

Figure A3. 50-year running mean of Wetland methane emissions vs. global average temperature anomaly for each scenario run in (Kleinen et al., 2021a).

Coverage	**Slope [Mt/K]**
Zhang *et al.* (2017)	
2000-2100	35.5
Kleinen *et al.* (2021)	
1850-2300	52.6
1850-2500	45.8
1850-3000	37.4

Table A1. Slopes fit to the respective model data.

Category	Mean Years Above 1.5°C (Std Dev)		Mean Integral above Overshoot [Degree-Years] (Std Dev)	
	v7.5.3	**v7.6**	**v7.5.3**	**v7.6**
C1	28.7 (13.8)	38.9 (15.9)	1.5 (1.0)	2.7 (1.6)
C2	53.3 (10.8)	59.8 (9.8)	7.0 (3.1)	9.3 (3.6)

Table A2. Summary statistics of the overshoot scenarios in the AR6 C1 and C2 categories. For both versions of MAGICC, the total number of years above 1.5°C and the integral of the curve above 1.5° were calculated for all scenarios, with the means (and standard deviations) presented above.

https://doi.org/10.5194/egusphere-2025-3873
Preprint. Discussion started: 5 September 2025

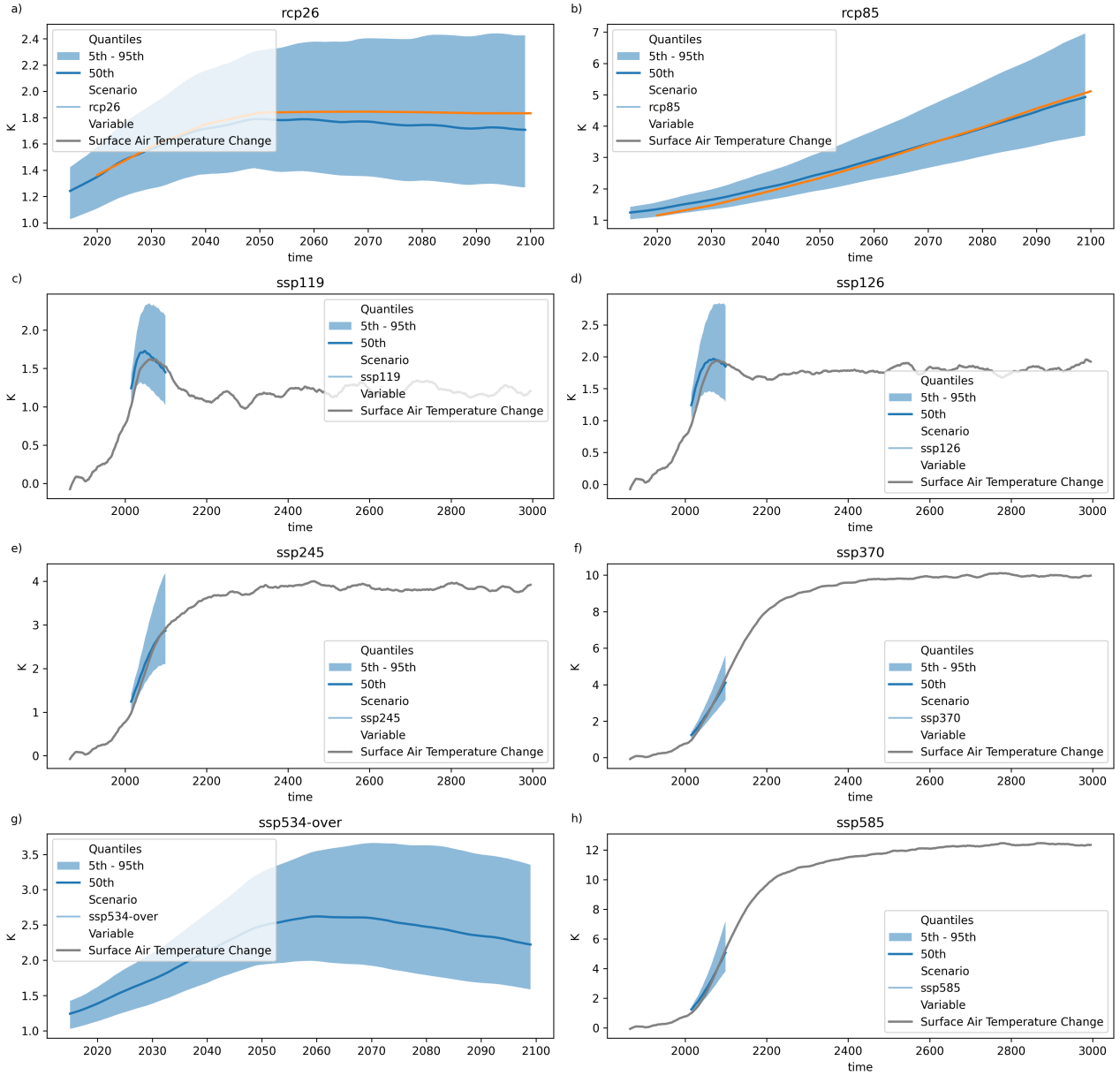

Figure A4. Comparison of temperature data in Zhang et al. (2017) and Kleinen et al. (2021a) with the outputs from the same scenarios in MAGICC v7.6. The Kleinen *et al.* runs extend to 3000, while the Zhang *et al.* and the MAGICC runs end in 2100.

https://doi.org/10.5194/egusphere-2025-3873
Preprint. Discussion started: 5 September 2025

Model	Scenario	Median EOC Warming [°C]
AIM/CGE 2.2	EN_NPi2020_600	1.527
COFFEE 1.1	EN_NPi2020_400	1.541
GCAM 5.3	R_MAC_30_n0	1.526
REMIND 2.1	CEMICS_opt_1p5	1.509
REMIND-MAgPIE 2.1-4.2	EN_NPi2020_600	1.500
REMIND-MAgPIE 2.1-4.2	EN_NPi2020_600_COV	1.501
REMIND-MAgPIE 2.1-4.2	EN_NPi2020_600f_COV	1.509
WITCH 5.0	EN_NPi2020_500	1.510
WITCH 5.0	EN_NPi2020_500f	1.521

Table A3. C1 Scenarios which no longer meet the criteria of staying below 1.5°C warming in 2100 with a 50% probability.

https://doi.org/10.5194/egusphere-2025-3873
Preprint. Discussion started: 5 September 2025

Model	Scenario	Median EOC Warming [°C]
AIM/CGE 2.2	EN_NPi2020_600f	1.527
COFFEE 1.1	EN_INDCi2030_500f	1.515
	EN_NPi2020_500f	1.507
GCAM 5.3	R_MAC_60_n8	1.537
GEM-E3_V2021	EN_INDCi2030_800f	1.560
	EN_NPi2020_600	1.524
MESSAGE-GLOBIOM 1.0	EMF30_Slower-to-faster	1.510
MESSAGEix-GLOBIOM_1.1	EN_NPi2020_700	1.536
	EN_NPi2020_700_COV	1.5306
	EN_NPi2020_700f	1.516
	EN_NPi2020_700f_COV	1.515
MESSAGEix-GLOBIOM_GEI 1.0	SSP2_int_mc_50	1.549
	SSP2_noint_mc_50	1.553
	SSP2_openres_mc_50	1.5478
POLES ADVANCE	ADVANCE_2020_WB2C	1.502
POLES ENGAGE	EN_INDCi2030_400f	1.532
	EN_NPi2020_300f	1.504
	EN_NPi2020_400f	1.512
REMIND 2.1	LeastTotalCost_LTC_brkSR15_SSP1_P50	1.513
	R2p1_SSP5-PkBudg1100	1.511
REMIND-MAgPIE 1.7-3.0	CD-LINKS_INDC2030i_1000	1.510
	CD-LINKS_NPi2020_1000	1.503
	CO_Bridge	1.509
	PEP_2C_full_netzero	1.502
REMIND-MAgPIE 2.1-4.2	EN_INDCi2030_600_COV	1.503
	EN_INDCi2030_600_COV_NDCp	1.502
	EN_INDCi2030_600f	1.550
	EN_INDCi2030_600f_COV	1.546
	EN_INDCi2030_600f_COV_NDCp	1.546
	EN_INDCi2030_600f_NDCp	1.549
	EN_NPi2020_600f	1.515
REMIND-MAgPIE 2.1-4.3	DeepElec_SSP2_def_Budg1100	1.504
WITCH 5.0	EN_INDCi2030_500f	1.545

Table A4. C2 Scenarios which no longer meet the criteria of staying below 1.5°C warming in 2100 with a 50% probability.

https://doi.org/10.5194/egusphere-2025-3873
Preprint. Discussion started: 5 September 2025

Model	Scenario	Peak Temperature [°C]
AIM/CGE 2.2	EN_INDCi2030_1000f	2.037
AIM/CGE 2.2	EN_NPi2020_1000f	2.039
AIM/CGE 2.2	EN_NPi2020_1200	2.033
COFFEE 1.1	CO_Bridge	2.035
COFFEE 1.1	EN_INDCi2030_900	2.027
COFFEE 1.1	EN_NPi2020_900	2.058
GCAM 5.3	R_MAC_65_n0	2.036
GCAM 5.3	R_MAC_75_n8	2.008
GEM-E3_V2021	EN_INDCi2030_1000	2.003
GEM-E3_V2021	EN_INDCi2030_1000_NDCp	2.000
GEM-E3_V2021	EN_INDCi2030_1000f_COV	2.011
GEM-E3_V2021	EN_INDCi2030_1000f_COV_NDCp	2.002
GEM-E3_V2021	EN_NPi2020_1000	2.019
GEM-E3_V2021	EN_NPi2020_1000_COV	2.003
GEM-E3_V2021	EN_NPi2020_1000f_COV	2.030
GEM-E3_V2021	EN_NPi2020_800f	2.005
IMAGE 3.0	CO_2Deg2030	2.024
IMAGE 3.0	EN_NPi2020_1000f	2.019
IMAGE 3.0.1	CD-LINKS_NDC2030i_1000	2.033
IMAGE 3.0.1	EMF30_Slower-to-faster+SLCF	2.053
IMAGE 3.0.1	EMF30_Slower-to-faster+SLCF+HFC	2.049
IMAGE 3.0.1	SSP1-26	2.010
IMAGE 3.0.2	EMF33_WB2C_full	2.004
IMAGE 3.0.2	EMF33_WB2C_nobeccs	2.059
IMAGE 3.2	SSP1_SPA1_26I_LIRE	2.001
IMAGE 3.2	SSP2_SPA2_26I_RE	2.012

Table A5. C3 Scenarios which no longer meet the criteria of staying below 2°C peak warming with a 67% probability.

https://doi.org/10.5194/egusphere-2025-3873
Preprint. Discussion started: 5 September 2025

Model	Scenario	Peak Temperature [°C]
MESSAGEix-GLOBIOM_1.1	EN_INDCi2030_1000f_COV	2.041
MESSAGEix-GLOBIOM_1.1	EN_INDCi2030_1000f_COV_NDCp	2.036
MESSAGEix-GLOBIOM_1.1	EN_INDCi2030_1200_COV	2.043
MESSAGEix-GLOBIOM_1.1	EN_INDCi2030_1200_COV_NDCp	2.041
MESSAGEix-GLOBIOM_1.1	EN_INDCi2030_800f	2.006
MESSAGEix-GLOBIOM_1.1	EN_INDCi2030_800f_NDCp	2.002
MESSAGEix-GLOBIOM_1.1	EN_INDCi2030_900f	2.037
MESSAGEix-GLOBIOM_1.1	EN_INDCi2030_900f_COV	2.010
MESSAGEix-GLOBIOM_1.1	EN_INDCi2030_900f_COV_NDCp	2.002
MESSAGEix-GLOBIOM_1.1	EN_INDCi2030_900f_NDCp	2.031
MESSAGEix-GLOBIOM_1.1	EN_INDCi2030_950f_COV	2.025
MESSAGEix-GLOBIOM_1.1	EN_INDCi2030_950f_COV_NDCp	2.017
MESSAGEix-GLOBIOM_1.1	EN_NPi2020_1000f	2.031
MESSAGEix-GLOBIOM_1.1	EN_NPi2020_1000f_COV	2.005
MESSAGEix-GLOBIOM_1.1	EN_NPi2020_1000f_DR4p	2.008
MESSAGEix-GLOBIOM_1.1	EN_NPi2020_1200	2.046
MESSAGEix-GLOBIOM_1.1	EN_NPi2020_1200_COV	2.031
MESSAGEix-GLOBIOM_GEI 1.0	SSP2_openres_lc_50	2.003
POLES ADVANCE	ADVANCE_2020_Med2C	2.057
POLES ADVANCE	ADVANCE_2030_Med2C	2.052
POLES ENGAGE	EN_INDCi2030_600f	2.024
POLES ENGAGE	EN_INDCi2030_700f	2.043
POLES ENGAGE	EN_INDCi2030_900	2.049
POLES ENGAGE	EN_NPi2020_700f	2.003
POLES ENGAGE	EN_NPi2020_800	2.025
POLES ENGAGE	EN_NPi2020_900	2.034
POLES GECO2019	CO_2Deg2020	2.023
POLES GECO2019	CO_2Deg2030	2.031

Table A6. C3 Scenarios which no longer meet the criteria of staying below 2°C peak warming with a 67% probability (*cont'd*).

https://doi.org/10.5194/egusphere-2025-3873
Preprint. Discussion started: 5 September 2025

Model	Scenario	Peak Temperature [°C]
REMIND 1.6	EMF30_Slower-to-faster	2.047
REMIND 1.6	EMF30_Slower-to-faster+SLCF	2.001
REMIND 1.6	EMF30_Slower-to-faster+SLCF+HFC	2.001
REMIND 1.7	ADVANCE_2020_Med2C	2.005
REMIND 2.1	LeastTotalCost_CBA_brkSR15_SSP2_P50	2.013
REMIND-MAgPIE 1.5	SSP2-26	2.043
REMIND-MAgPIE 1.7-3.0	EMF33_Med2C_limbio	2.070
REMIND-MAgPIE 1.7-3.0	EMF33_WB2C_cost100	2.011
REMIND-MAgPIE 1.7-3.0	EMF33_WB2C_full	2.019
REMIND-MAgPIE 1.7-3.0	EMF33_tax_hi_full	2.025
REMIND-MAgPIE 2.0-4.1	Diff_1300Gt_hybrid_def	2.011
REMIND-MAgPIE 2.0-4.1	Diff_1300Gt_no-transfer_def	2.048
REMIND-MAgPIE 2.0-4.1	Diff_1300Gt_uniform-pricing_def	2.004
REMIND-MAgPIE 2.1-4.2	EN_INDCi2030_1200	2.008
REMIND-MAgPIE 2.1-4.2	EN_INDCi2030_1200f	2.008
REMIND-MAgPIE 2.1-4.2	EN_NPi2020_1200	2.034
REMIND-MAgPIE 2.1-4.2	EN_NPi2020_1200f	2.032
TIAM-ECN 1.1	EN_INDCi2030_1200	2.045
TIAM-ECN 1.1	EN_INDCi2030_1200f	2.037
TIAM-ECN 1.1	EN_NPi2020_1200	2.018
TIAM-ECN 1.1	EN_NPi2020_1200f	2.030
WITCH 5.0	EN_INDCi2030_1000	2.037
WITCH 5.0	EN_INDCi2030_1000_NDCp	2.020
WITCH 5.0	EN_INDCi2030_1000f	2.070
WITCH 5.0	EN_INDCi2030_1000f_NDCp	2.069
WITCH 5.0	EN_INDCi2030_900f	2.028
WITCH 5.0	EN_INDCi2030_900f_NDCp	2.024
WITCH 5.0	EN_NPi2020_1000f	2.028

Table A7. C3 Scenarios which no longer meet the criteria of staying below 2°C peak warming with a 67% probability (*cont'd*)

https://doi.org/10.5194/egusphere-2025-3873
Preprint. Discussion started: 5 September 2025

Code and data availability. The current version of MAGICC v7.6 is available from the project website https://doi.org/10.5281/zenodo.17054564 under the Creative Commons Attribution 4.0 International License (CC BY 4.0). The exact version of the probabilistic distribution used to produce the results used in this paper is archived on repository under https://doi.org/10.5281/zenodo.14678474 (Sloughter and Nicholls, 2025). The data from (Kleinen et al., 2021a) is available from the World Data Center for Climate (WDCC) at DKRZ (Kleinen et al., 2021b). The data from (Zhang et al., 2017) is available on the article website.

Author contributions. TS performed the data analysis, calibration, and updates to the code under supervision of ZN and JR and with input from GT, TK, and ZZ. ZN provided template notebooks for the calibration. TK and ZZ provided the data for analysis and gave feedback on the model development. TS wrote the first draft of this paper, all co-authors reviewed and edited the whole of the manuscript.

Competing interests. The contact author has declared that none of the authors has any competing interests.

Acknowledgements. Trevor Sloughter acknowledges support from the project ESM2025 which received funding from the European Union's Horizon 2020 research and innovation programme under grant agreement No. 101003536. Thomas Kleinen acknowledges support from the PalMod project, funded by the German Federal Ministry of Education and Research (BMBF) (01LP1921A), and from the European Research Council (ERC) under the European Union's Horizon 2020 research and innovation program (grant agreement No. 951288, Q-Arctic).

https://doi.org/10.5194/egusphere-2025-3873
Preprint. Discussion started: 5 September 2025

References

Byers, E., Krey, V., Kriegler, E., Riahi, K., Schaeffer, R., Kikstra, J., Lamboll, R., Nicholls, Z., Sandstad, M., Smith, C., van der Wijst, K., Al Khourdajie, A., Lecocq, F., Portugal-Pereira, J., Saheb, Y., Stromman, A., Winkler, H., Auer, C., Brutschin, E., Gidden, M., Hackstock, P., Harmsen, M., Huppmann, D., Kolp, P., Lepault, C., Lewis, J., Marangoni, G., Müller-Casseres, E., Skeie, R., Werning, M., Calvin, K., Forster, P., Guivarch, C., Hasegawa, T., Meinshausen, M., Peters, G., Rogelj, J., Samset, B., Steinberger, J., Tavoni, M., and van Vuuren, D.: AR6 Scenarios Database, https://doi.org/10.5281/zenodo.7197970, 2022.

Chang, K.-Y., Riley, W. J., Knox, S. H., Jackson, R. B., McNicol, G., Poulter, B., Aurela, M., Baldocchi, D., Bansal, S., Bohrer, G., et al.: Substantial hysteresis in emergent temperature sensitivity of global wetland CH4 emissions, Nature Communications, 12, 2266, 2021.

Davidson, N. C., Fluet-Chouinard, E., and Finlayson, C. M.: Global extent and distribution of wetlands: trends and issues, Marine and Freshwater Research, 69, 620–627, 2018.

Folberth, G., Staniaszek, Z., Archibald, A., Gedney, N., Griffiths, P., Jones, C., O'connor, F., Parker, R., Sellar, A., and Wiltshire, A.: Description and evaluation of an emission-driven and fully coupled methane cycle in UKESM1, Journal of Advances in Modeling Earth Systems, 14, e2021MS002 982, 2022.

Forster, P., Storelvmo, T., Armour, K., Collins, W., Dufresne, J.-L., Frame, D., Lunt, D., Mauritsen, T., Palmer, M., Watanabe, M., Wild, M., and Zhang, H.: The Earth's Energy Budget, Climate Feedbacks, and Climate Sensitivity, in: Climate Change 2021: The Physical Science Basis. Contribution of Working Group I to the Sixth Assessment Report of the Intergovernmental Panel on Climate Change, edited by Masson-Delmotte, V., Zhai, P., Pirani, A., Connors, S. L., Péan, C., Berger, S., Caud, N., Chen, Y., Goldfarb, L., Gomis, M. I., Huang, M., Leitzell, K., Lonnoy, E., Matthews, J. B. R., Maycock, T. K., Waterfield, T., Yelekçi, O., Yu, R., and Zhou, B., book section 7, pp. 923–1054, Cambridge University Press, Cambridge, UK and New York, NY, USA, https://doi.org/10.1017/9781009157896.009, 2021.

Gedney, N., Huntingford, C., Comyn-Platt, E., and Wiltshire, A.: Significant feedbacks of wetland methane release on climate change and the causes of their uncertainty, Environmental Research Letters, 14, 084 027, 2019.

Im, U., Tsigaridis, K., Bauer, S. E., Shindell, D. T., Olivié, D., Wilson, S., Sørensen, L. L., Langen, P. L., and Eckhardt, S.: Future CH4 as modelled by a fully coupled Earth system model: prescribed GHG concentrations vs. interactive CH4 sources and sinks, Environmental Research: Climate, 2025.

Kikstra, J. S., Nicholls, Z. R., Smith, C. J., Lewis, J., Lamboll, R. D., Byers, E., Sandstad, M., Meinshausen, M., Gidden, M. J., Rogelj, J., et al.: The IPCC Sixth Assessment Report WGIII climate assessment of mitigation pathways: from emissions to global temperatures, Geoscientific Model Development, 15, 9075–9109, 2022.

Kleinen, T., Gromov, S., Steil, B., and Brovkin, V.: Atmospheric methane underestimated in future climate projections, Environmental Research Letters, 16, 094 006, 2021a.

Kleinen, T., Gromov, S., Steil, B., and Brovkin, V.: Natural methane emissions 1850-3009, https://hdl.handle.net/21.14106/edf716626b6105380067d7eeece2e4020464c793, 2021b.

Kleinen, T., Gromov, S., Steil, B., and Brovkin, V.: Atmospheric methane since the last glacial maximum was driven by wetland sources, Climate of the Past, 19, 1081–1099, 2023.

Mauritsen, T., Bader, J., Becker, T., Behrens, J., Bittner, M., Brokopf, R., Brovkin, V., Claussen, M., Crueger, T., Esch, M., et al.: Developments in the MPI-M Earth System Model version 1.2 (MPI-ESM1. 2) and its response to increasing CO2, Journal of Advances in Modeling Earth Systems, 11, 998–1038, 2019.

https://doi.org/10.5194/egusphere-2025-3873
Preprint. Discussion started: 5 September 2025

Meinshausen, M., Raper, S. C., and Wigley, T. M.: Emulating coupled atmosphere-ocean and carbon cycle models with a simpler model, MAGICC6–Part 1: Model description and calibration, Atmospheric Chemistry and Physics, 11, 1417–1456, 2011a.

Meinshausen, M., Smith, S. J., Calvin, K., Daniel, J. S., Kainuma, M. L., Lamarque, J.-F., Matsumoto, K., Montzka, S. A., Raper, S. C., Riahi, K., et al.: The RCP greenhouse gas concentrations and their extensions from 1765 to 2300, Climatic change, 109, 213, 2011b.

Meinshausen, M., Wigley, T., and Raper, S.: Emulating atmosphere-ocean and carbon cycle models with a simpler model, MAGICC6–Part 2: Applications, Atmospheric Chemistry and Physics, 11, 1457–1471, 2011c.

Meinshausen, M., Nicholls, Z. R., Lewis, J., Gidden, M. J., Vogel, E., Freund, M., Beyerle, U., Gessner, C., Nauels, A., Bauer, N., et al.: The shared socio-economic pathway (SSP) greenhouse gas concentrations and their extensions to 2500, Geoscientific Model Development, 13, 3571–3605, 2020.

Nelder, J. A. and Mead, R.: A simplex method for function minimization, The computer journal, 7, 308–313, 1965.

Nicholls, Z., Meinshausen, M., Lewis, J., Corradi, M. R., Dorheim, K., Gasser, T., Gieseke, R., Hope, A. P., Leach, N., McBride, L., et al.: Reduced complexity model intercomparison project phase 2: synthesizing earth system knowledge for probabilistic climate projections, Earth's Future, 9, e2020EF001 900, 2021.

Nicholls, Z., Meinshausen, M., and Lewis, J.: MAGICC7 SSP carbon cycle output using AR6 tuning, 2023.

Nicholls, Z., Lewis, J., Tang, G., Trevor, S., Nauels, A., Norton, A., Wigley, T., and Meinshausen, M.: Model for the Assessment of Greenhouse gas Induced Climate Change (MAGICC), https://doi.org/10.5281/zenodo.17054564, 2025.

O'Neill, B. C., Tebaldi, C., Van Vuuren, D. P., Eyring, V., Friedlingstein, P., Hurtt, G., Knutti, R., Kriegler, E., Lamarque, J.-F., Lowe, J., et al.: The scenario model intercomparison project (ScenarioMIP) for CMIP6, Geoscientific Model Development, 9, 3461–3482, 2016.

Peng, S., Lin, X., Thompson, R. L., Xi, Y., Liu, G., Hauglustaine, D., Lan, X., Poulter, B., Ramonet, M., Saunois, M., et al.: Wetland emission and atmospheric sink changes explain methane growth in 2020, Nature, 612, 477–482, 2022.

Qu, Z., Jacob, D. J., Bloom, A. A., Worden, J. R., Parker, R. J., and Boesch, H.: Inverse modeling of 2010–2022 satellite observations shows that inundation of the wet tropics drove the 2020–2022 methane surge, Proceedings of the National Academy of Sciences, 121, e2402730 121, 2024.

Riahi, K., Van Vuuren, D. P., Kriegler, E., Edmonds, J., O'neill, B. C., Fujimori, S., Bauer, N., Calvin, K., Dellink, R., Fricko, O., et al.: The Shared Socioeconomic Pathways and their energy, land use, and greenhouse gas emissions implications: An overview, Global environmental change, 42, 153–168, 2017.

Riahi, K., Schaeffer, R., Arango, J., Calvin, K., Guivarch, C., Hasegawa, T., Jiang, K., Kriegler, E., Matthews, R., Peters, G., Rao, A., Robertson, S., Sebbit, A., Steinberger, J., Tavoni, M., and Van Vuuren, D.: Mitigation pathways compatible with long-term goals, in: Climate Change 2022: Mitigation of Climate Change. Contribution of Working Group III to the Sixth Assessment Report of the Intergovernmental Panel on Climate Change, edited by Shukla, P., Skea, J., Slade, R., Khourdajie, A. A., van Diemen, R., McCollum, D., Pathak, M., Some, S., Vyas, P., Fradera, R., Belkacemi, M., Hasija, A., Lisboa, G., Luz, S., and Malley, J., book section 3, Cambridge University Press, Cambridge, UK and New York, NY, USA, https://doi.org/10.1017/9781009157926.005, 2022.

Sanderson, B. M., Booth, B. B., Dunne, J., Eyring, V., Fisher, R. A., Friedlingstein, P., Gidden, M. J., Hajima, T., Jones, C. D., Jones, C. G., et al.: The need for carbon-emissions-driven climate projections in CMIP7, Geoscientific Model Development, 17, 8141–8172, 2024.

Saunois, M., Stavert, A. R., Poulter, B., Bousquet, P., Canadell, J. G., Jackson, R. B., Raymond, P. A., Dlugokencky, E. J., Houweling, S., Patra, P. K., Ciais, P., Arora, V. K., Bastviken, D., Bergamaschi, P., Blake, D. R., Brailsford, G., Bruhwiler, L., Carlson, K. M., Carrol, M., Castaldi, S., Chandra, N., Crevoisier, C., Crill, P. M., Covey, K., Curry, C. L., Etiope, G., Frankenberg, C., Gedney, N., Hegglin, M. I., Höglund-Isaksson, L., Hugelius, G., Ishizawa, M., Ito, A., Janssens-Maenhout, G., Jensen, K. M., Joos, F., Kleinen, T., Krummel,

https://doi.org/10.5194/egusphere-2025-3873
Preprint. Discussion started: 5 September 2025

P. B., Langenfelds, R. L., Laruelle, G. G., Liu, L., Machida, T., Maksyutov, S., McDonald, K. C., McNorton, J., Miller, P. A., Melton, J. R., Morino, I., Müller, J., Murguia-Flores, F., Naik, V., Niwa, Y., Noce, S., O'Doherty, S., Parker, R. J., Peng, C., Peng, S., Peters, G. P., Prigent, C., Prinn, R., Ramonet, M., Regnier, P., Riley, W. J., Rosentreter, J. A., Segers, A., Simpson, I. J., Shi, H., Smith, S. J., Steele, L. P., Thornton, B. F., Tian, H., Tohjima, Y., Tubiello, F. N., Tsuruta, A., Viovy, N., Voulgarakis, A., Weber, T. S., van Weele, M., van der Werf, G. R., Weiss, R. F., Worthy, D., Wunch, D., Yin, Y., Yoshida, Y., Zhang, W., Zhang, Z., Zhao, Y., Zheng, B., Zhu, Q., Zhu, Q., and Zhuang, Q.: The Global Methane Budget 2000–2017, Earth System Science Data, 12, 1561–1623, https://doi.org/10.5194/essd-12-1561-2020, 2020.

Saunois, M., Martinez, A., Poulter, B., Zhang, Z., Raymond, P., Regnier, P., Canadell, J. G., Jackson, R. B., Patra, P. K., Bousquet, P., Ciais, P., Dlugokencky, E. J., Lan, X., Allen, G. H., Bastviken, D., Beerling, D. J., Belikov, D. A., Blake, D. R., Castaldi, S., Crippa, M., Deemer, B. R., Dennison, F., Etiope, G., Gedney, N., Höglund-Isaksson, L., Holgerson, M. A., Hopcroft, P. O., Hugelius, G., Ito, A., Jain, A. K., Janardanan, R., Johnson, M. S., Kleinen, T., Krummel, P., Lauerwald, R., Li, T., Liu, X., McDonald, K. C., Melton, J. R., Mühle, J., Müller, J., Murguia-Flores, F., Niwa, Y., Noce, S., Pan, S., Parker, R. J., Peng, C., Ramonet, M., Riley, W. J., Rocher-Ros, G., Rosentreter, J. A., Sasakawa, M., Segers, A., Smith, S. J., Stanley, E. H., Thanwerdas, J., Tian, H., Tsuruta, A., Tubiello, F. N., Weber, T. S., van der Werf, G., Worthy, D. E., Xi, Y., Yoshida, Y., Zhang, W., Zheng, B., Zhu, Q., Zhu, Q., and Zhuang, Q.: Global Methane Budget 2000–2020, Earth System Science Data Discussions, 2024, 1–147, https://doi.org/10.5194/essd-2024-115, 2024.

Shindell, D., Sadavarte, P., Aben, I., Bredariol, T. d. O., Dreyfus, G., Höglund-Isaksson, L., Poulter, B., Saunois, M., Schmidt, G. A., Szopa, S., et al.: The methane imperative, Frontiers in Science, 2, 1349 770, 2024.

Skeie, R. B., Hodnebrog, Ø., and Myhre, G.: Trends in atmospheric methane concentrations since 1990 were driven and modified by anthropogenic emissions, Communications Earth & Environment, 4, 317, 2023.

Sloughter, T. and Nicholls, Z.: MAGICC AR7 fast track probabilistic distribution, https://doi.org/10.5281/zenodo.14678474, 2025.

Tebaldi, C., Debeire, K., Eyring, V., Fischer, E., Fyfe, J., Friedlingstein, P., Knutti, R., Lowe, J., O'Neill, B., Sanderson, B., et al.: Climate model projections from the scenario model intercomparison project (ScenarioMIP) of CMIP6, Earth System Dynamics, 12, 253–293, 2021.

Zhang, Z., Zimmermann, N. E., Stenke, A., Li, X., Hodson, E. L., Zhu, G., Huang, C., and Poulter, B.: Emerging role of wetland methane emissions in driving 21st century climate change, Proceedings of the National Academy of Sciences, 114, 9647–9652, 2017.

Zhang, Z., Poulter, B., Feldman, A. F., Ying, Q., Ciais, P., Peng, S., and Li, X.: Recent intensification of wetland methane feedback, Nature Climate Change, 13, 430–433, 2023.

Zhang, Z., Poulter, B., Melton, J. R., Riley, W. J., Allen, G. H., Beerling, D. J., Bousquet, P., Canadell, J. G., Fluet-Chouinard, E., Ciais, P., et al.: Ensemble estimates of global wetland methane emissions over 2000–2020, Biogeosciences, 22, 305–321, 2025.

Zhu, B., Qiu, C., Gasser, T., Ciais, P., Lamboll, R. D., Ballantyne, A., Chang, J., Gallego-Sala, A. V., Guenet, B., Holden, J., et al.: Warming of Northern Peatlands Increases the Global Temperature Overshoot Challenge, Authorea Preprints, 2024.